

ARTICLE

Open Access



Design, synthesis, and biological evaluation of chalcones for anticancer properties targeting glycogen synthase kinase 3 beta

Seunghyun Ahn¹, Vi Nguyen-Phuong Truong², Beomsoo Kim³, Miri Yoo¹, Yoongho Lim³, Somi Kim Cho^{2*} and Dongsoo Koh^{1*} 

Abstract

Chalcones compounds have been investigated to exhibit anticancer activity through various physiological modes of action. In order to develop chalcone compounds with novel anticancer-related modes of action, diverse chalcone compounds were designed and synthesized. Various substituted poly-methoxy chalcone compounds **1–17** were prepared, and their structures were identified using high-resolution mass spectrometry (HR/MS) and nuclear magnetic resonance (NMR) experiments. Long-term survival clonogenic assay was applied to evaluate their anti-cancer abilities and revealed that their GI₅₀ values ranged between 1.33 and 172.20 μM . When MCF-7SC cells were treated with various concentrations of compound **14**, reduced cell viability and induced apoptosis in MCF-7SC cells were observed in a dose-dependent manner. Wound healing assay demonstrated that compound **14** prevented the MCF-7SC migrated cells at non-lethal concentrations after 12 and 24 h of exposure. The efficiency of compound **14** on the levels of Epithelial-mesenchymal transition (EMT) markers was accessed by the western blot analysis. For the concrete understanding of anticancer properties at the molecular level, in vitro kinase assays on 12 cancer related proteins were carried out. Glycogen synthase kinase 3 beta (GSK3 β) was most effectively inhibited by compound **14** with 89% inhibitory activity at 10 μM against GSK3 β . The binding mode of compound **14** with GSK3 β was reinforced through in silico experiments, which demonstrated compound **14** binds with GSK3 β at binding affinity ranged between -7.5 kcal/mol and -6.8 kcal/mol. SwissADME analysis provided the druggability and leadlikeness of compound **14**, which unveiled drug development possibilities of chalcone compound **14**.

Keywords: Chalcone, Clonogenic, MCF-7SC, GSK3 β , In silico docking

Introduction

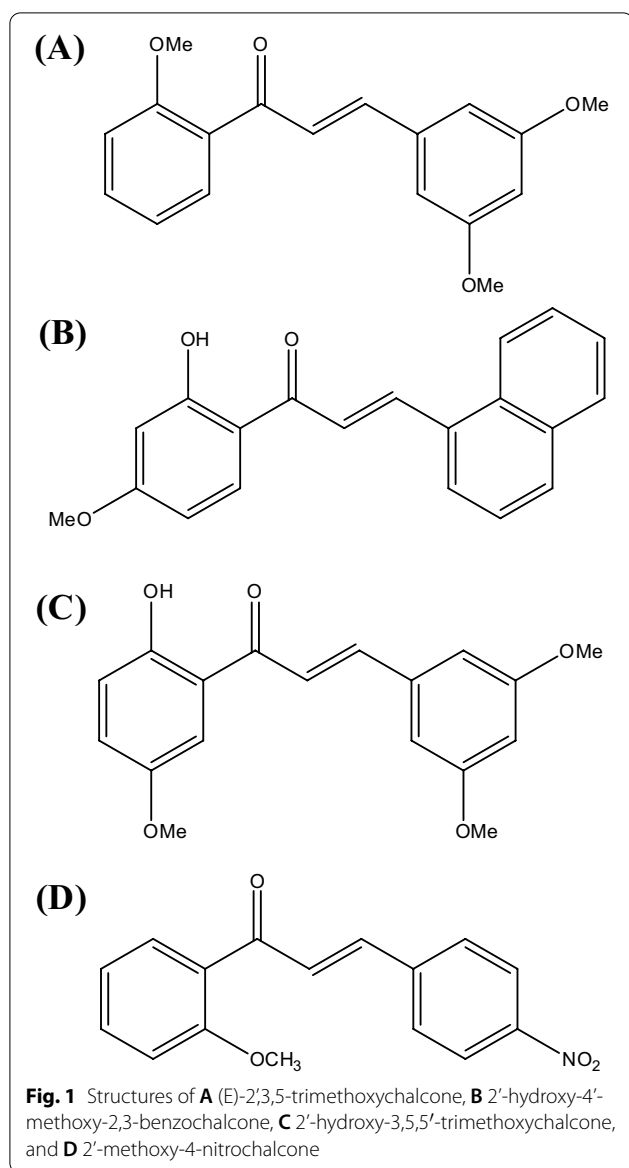
Chalcones have a common skeleton, 1,3-diaryl-2-propen-1-one. Because benzene rings can be substituted, various compounds have been reported. They are known to show diverse biological activities including antituberculosis, antidiabetic, antimicrobial, antimalarial, anti-inflammatory, anticancer activities, and so on [1–6]. In

our previous research, chalcone compounds have anticancer effects. (E)-2',3,5-trimethoxychalcone (Fig. 1A) induced apoptosis and inhibited the cancer cell growth via the reactive oxygen species (ROS) generation [7]. 2'-Hydroxy-4'-methoxy-2,3-benzochalcone (Fig. 1B) showed inhibitory effect on clonogenicity of Capan-1 human pancreatic cancer cells based on G2/M phase cell cycle arrest [8]. 2'-Hydroxy-3,5,5'-trimethoxychalcone (Fig. 1C) caused reactive oxygen species-induced apoptosis [9], and induced unfolded protein response-mediated apoptosis [10]. As mentioned above, anticancer effects of chalcones occur through various pathways. To find compounds showing anticancer activities, chalcone

*Correspondence: phd.kim.somi@gmail.com; dskoh@dongduk.ac.kr

¹ Department of Applied Chemistry, Dongduk Women's University, Seoul 02748, South Korea

² Interdisciplinary Graduate Program in Advanced Convergence Technology and Science, Jeju National University, Jeju 63243, South Korea
Full list of author information is available at the end of the article



compounds with poly-methoxy substituted chalcone derivatives were designed and synthesized. They were identified using $^1\text{H-NMR}$, $^{13}\text{C-NMR}$ 2D-NMR spectroscopy and HR/MS spectrometry. Their anticancer activities were measured based on cytotoxicities against cancer cell lines. The cytotoxicities were determined using a long-term survival clonogenic assay. Because 2'-methoxy-4-nitrochalcone (compound **14**) (Fig. 1D) showed the best cell growth inhibitory effect and good solubility, it was selected for further experiments.

Breast cancer is recognized as the most common type of cancer for women worldwide, and it is estimated that by 2040, breast cancer cases will increase by more than 46% [11]. Although many therapeutic strategies have been

established for the treatment of breast cancer, including surgery, chemotherapy, radiation therapy, and hormone therapy, however, these existing therapies have some limitations [12]. The main causes of breast cancer treatment failure, such as resistance to chemotherapy and radiotherapy, recurrence, metastasis, and weak immune monitoring, can be explained by the characteristics of cancer stem cells (CSC) [13, 14]. Therefore, CSC has become a promising therapeutic target in the treatment of breast cancer [15, 16]. There are several reports to identify CSC signatures, such as CD34+/CD38-, CD44-/CD24+ population, the enrichment of abnormal signaling like Wnt/ β -catenin, NF- κ B, or Notch pathways, promoting metastasis and tumor progression [17]. Furthermore, members of the ATP binding cassette (ABC) transporter subfamily, such as multidrug resistance protein 1 (ABCB1/MDR1) or multidrug resistance-associated protein 1 (ABCC1/MRP1) are overexpressed in different cancers, driving chemotherapy resistance and CSC biological function [18]. The stem-like MCF-7/SC cells, which is isolated from human breast carcinoma MCF-7 cells, possessed an up-regulated CD44+/CD24 population, overexpressed drug efflux protein MRP1, and possessed features such as increased migration capacity [19]. The anticancer activity of the compound was investigated by measuring the effects on cell proliferation, apoptosis induction, epithelial-mesenchymal transition, and stem cell potential of MCF-7SC cells, which have higher stem cell characteristics compared to the parental MCF-7 cells.

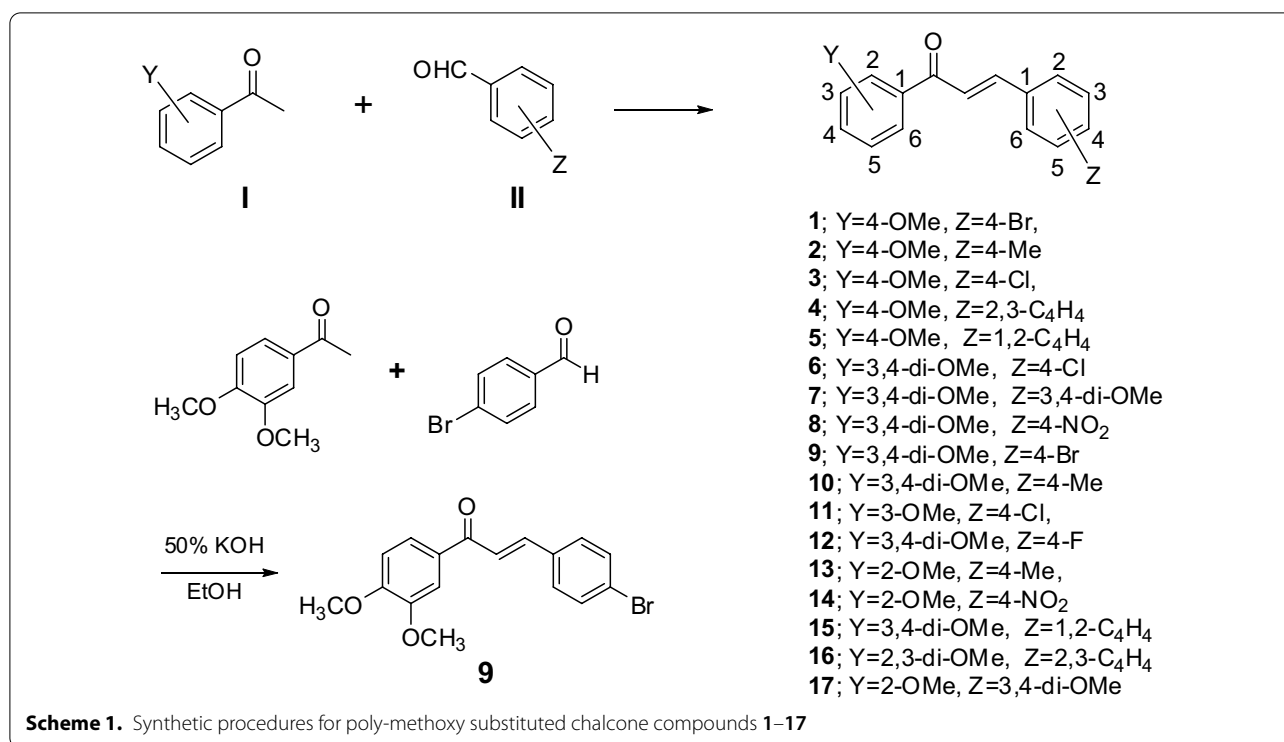
To understand the results obtained from the biological experiments mentioned above at the molecular level, in vitro kinase assays were carried out. Of several kinases, glycogen synthase kinase 3 beta (GSK3 β) was most effectively inhibited by compound **14**. To elucidate whether compound **14** binds to GSK3 β , in silico docking experiments were performed. The results obtained in this study demonstrated the compound **14** can be developed as a chemotherapeutic agent.

Materials and methods

Synthesis

Variously substituted poly-methoxy acetophenones (**I**) and substituted benzaldehydes (**II**) were used to obtain poly-methoxy substituted chalcone derivatives **1–17** as shown in Scheme 1. Typical procedure for preparation of compound **9** was described as an example.

4-bromobenzaldehyde (1 mmol, 184 mg) and 3,4-dimethoxyacetophenone (1 mmol, 180 mg) were dissolved in 20 ml of anhydrous ethanol and the reaction mixture was stirred around 275–276 K. After addition of aqueous KOH solution (50%, 1 ml) to the cooled reaction mixture, the reaction mixture was stirred at room



temperature for 20 h. After completion of the reaction (monitored by TLC), this mixture was poured into iced water (50 ml) and was acidified with 6 M HCl solution until pH = 2 to produce a solid product **9** in 54% yield.

Spectroscopic methods

The structures of the chalcone compounds synthesized here were determined using NMR spectroscopy and HR/MS spectrometry. The concentrations of the compounds dissolved in deuterated dimethyl sulfoxide were adjusted to approximately 50 mM. They were transferred into 2.5 mm NMR tubes to generate good spectra using short acquisition times. All NMR experiments were carried out on a Bruker AVANCE 400 spectrometer (9.4 Tesla) at room temperature. The detailed NMR experimental method followed the previous report [20]. HR/MS data were collected according to a previously published method in [M+H]⁺ mode using Waters ACQUITY UPLC (Waters, Milford, MA, USA) [21].

Biological experiments

Clonogenic assay

The clonogenic assay was used to access the long-term survival of cells as previously described [22]. Briefly, cells were seeded on 24-well plates and treated with increasing concentrations of different compounds. After seven days of incubation, colonies were fixed with 6% glutaraldehyde, followed by staining with 0.1%

crystal violet. Densitometry (MultiGuage, Fujifilm, Japan) was used to determine the cell growth inhibitory dosage values, and the SigmaPlot tool was used to calculate GI₅₀ values.

MTT assay

The MTT assay was used to access the cell viability. Briefly, cells (2 × 10⁴ cells/mL) were seeded into 96-well plates. After that, cells were treated with increasing concentration of compound **14** following 24 or 48 h of incubation. MTT reagent (1 mg/mL) was added to each well (ratio 1:4 with media) and incubated for 2–3 h at 37 °C. Then, 100 μL of Dimethyl sulfoxide (DMSO) was added to solubilize formazan crystals. The absorbance was recorded at 570 nm by a micro-plate reader (Tecan Group, Ltd., Salzburg, Austria).

Flow cytometric assay for CD44⁺/CD24⁻ population

Cells (1 × 10⁵ cells/mL) were seeded into 60 mm dishes and then treated with compound **14** for 24 h. After that, cells were exposed with immunofluorescence staining buffer (100 μL/sample) containing phytoerythrin-conjugated (PE) anti-human CD24 antibody (10 μL/sample) and fluorescein isothiocyanate-conjugated (FITC) anti-human CD44 antibody (10 μL/sample) (BD Pharmingen).

The CD44⁺/CD24⁻ population was detected by fluorescence-activated cell sorting (FACSCalibur).

Flow cytometric assay for Annexin V/PI staining

Cells (1×10^5 cells/mL) were seeded onto 60 mm plates and then treated with compound **14** at different doses. After 24 h of incubation, cells were washed with PBS and stained with an Annexin V-FITC Apoptosis Detection Kit (BD Pharmingen, San Diego, CA, USA) for 15 min at 37 °C to detect apoptotic population. FACSCalibur flow cytometer was used to access apoptotic cells.

Wound healing assay

Cells were cultured in 6-well cell culture plates and allowed to grow until cell density reached 95% confluence. A uniform scratch was made in each well by a 10 μ L sterile pipette tip and then, floating cells were washed with PBS. After that, cells were exposed to compound **14** at non-lethal dosage for 24 h. The widths of scratches were quantified under a phase contrast microscope (magnification at 100x).

Western blotting analysis

Cells were harvested by the radioimmunoprecipitation assay buffer (RIPA) buffer comprising protease inhibitor cocktail (PIC) and Phenylmethylsulfonyl fluoride—PMSF (Sigma-Aldrich, Missouri, USA). Protein concentration was quantified by the bicinchoninic acid assay (BCA) kit (Thermo Fisher Scientific, Waltham, MA, USA). After quantification, lysate was separated using sodium dodecyl sulphate–polyacrylamide gel electrophoresis (SDS-PAGE). Samples were then electrophoretic transferred to PVDF membranes, followed by blocking with 5% non-fat milk overnight. Primary antibodies were purchased from Cell Signaling Technology, Beverly, MA, USA, except the mouse anti-E-cadherin and β -catenin antibody (BD Transduction Laboratories, San Jose, CA, USA). The secondary antibodies (Vector Laboratories, Burlingame, CA, USA) were diluted at 1:5000 following the manufacturer's recommendations.

In vitro kinase assay

Kinase assays were performed according to a previously published method [22].

In silico docking

In silico docking experiments were carried out using AutoDock Vina (The Scripps Research Institute, La Jolla, San Diego, USA) [23]. Dozens of structures of GSK3 β were deposited in the protein data bank. Of them, 5f95.pdb was selected for in silico docking experiments because it contains 2-[(cyclopropylcarbonyl)amino]-N-(4-phenylpyridin-3-yl)pyridine-4-carboxamide including

biphenyl group as a ligand [24]. The organism of 5f95.pdb was Homo sapiens. The protein was overexpressed on baculovirus system. Its 3D structure was determined by X-ray crystallography. The apo-protein was prepared using the Chimera program [25]. The binding site was determined using the grid box provided by AutoDock Tools. The 3D structures of chalcone compounds were determined based on the X-ray crystallographic structure obtained from the previous work [26].

Statistical analysis

GraphPad Prism 8.0 software was used for statistical analysis in this present study. Data are presented as the mean \pm standard deviation (SD) of three independent experiments. One way analysis of variance (One-way ANOVA) with Dunnett's post hoc test was used for accessing the differences between groups. In all analyses, * $p < 0.05$ was considered to indicate a statistically significant.

Results and discussion

^1H NMR, ^{13}C NMR and 2D NMR were used to identify the chemical structure of the synthesized chalcone compounds. The complete assignments of chemical shift values, multiplicity, and coupling constants for each hydrogen present in each compound are summarized in Table 1. All synthesized chalcone compounds contain a conjugated enone group at the center of the molecule. In a C=C double bond, the carbon near the carbonyl C=O is assigned an α position and the carbon farther away is called the β position. For all compounds, the values of coupling constants between α hydrogen and β hydrogen ($J_{\text{H}\alpha\text{-H}\beta}$) range from 15.3 to 16 ppm, indicating that the carbon–carbon double bond is in the *trans* configuration. Table 2 shows the chemical shift values for all carbon atoms. In general, carbon in C=O is in the most down field region (187.2 to 192.5 ppm) of all carbons. It is noteworthy that the chemical shift values of all β carbons (119.6–130.6 ppm) always appear in the more down field region than the corresponding chemical shift values (139.0–143.5 ppm) of all α carbons.

To measure anticancer effects of chalcone compounds, cytotoxicity assays in cancer cell lines have been used. Here, a long-term survival clonogenic assay was used because it can distinguish activities caused by small structural differences. In order to obtain the half-maximal cell growth inhibitory concentration (GI₅₀) values, different concentrations of compounds (0, 10, 20, and 40 μ M) were treated in cancer cells. In the case of compounds **13** and **14**, which have good cell growth inhibitory effects, efficacy was confirmed at a low concentration of 10 μ M or less. The GI₅₀ data are shown in Fig. 2.

Table 1 $^1\text{H-NMR}$ data of compounds **1–17**

	1	2	3	4	5	6
H2	8.17(ddd, 8.8, 2.8, 1.9)	8.16(ddd, 8.8, 2.9, 1.9)	8.17(ddd, 8.8, 2.9, 1.9)	8.21(ddd, 8.9, 2.8, 1.9)	8.21(ddd, 8.9, 2.8, 1.9)	7.61(d, 2.0)
H3	7.08(ddd, 8.8, 2.8, 1.9)	7.08(ddd, 8.8, 2.9, 1.9)	7.09(ddd, 8.8, 2.9, 1.9)	7.11(ddd, 8.9, 2.8, 1.9)	7.11(ddd, 8.9, 2.8, 1.9)	–
H4	–	–	–	–	–	–
H5	7.08(ddd, 8.8, 2.8, 1.9)	7.08(ddd, 8.8, 2.9, 1.9)	7.09(ddd, 8.8, 2.9, 1.9)	7.11(ddd, 8.9, 2.8, 1.9)	7.11(ddd, 8.9, 2.8, 1.9)	7.10(d, 8.5)
H6	8.17(ddd, 8.8, 2.8, 1.9)	8.16(ddd, 8.8, 2.9, 1.9)	8.17(ddd, 8.8, 2.9, 1.9)	8.21(ddd, 8.9, 2.8, 1.9)	8.21(ddd, 8.9, 2.8, 1.9)	7.93(dd, 8.5, 2.0)
2-OMe	–	–	–	–	–	–
3-OMe	–	–	–	–	–	3.86(s)
4-OMe	3.87(s)	3.86(s)	3.87(s)	3.88(s)	3.88(s)	3.87(s)
H α	7.97(d, 15.6)	7.68(d, 15.6)	7.69(d, 15.6)	8.07(d, 15.5)	8.00(d, 15.3)	7.69(d, 15.6)
H β	7.67(d, 15.6)	7.88(d, 15.6)	7.96(d, 15.6)	7.88(d, 15.5)	8.54(d, 15.3)	7.97(d, 15.6)
H1'	–	–	–	8.32(d, 1.5)	–	–
H2'	7.84(ddd, 8.5, 2.5, 1.8)	7.76(d, 8.1)	7.91(ddd, 8.6, 2.5, 1.9)	–	8.23(d, 8.1)	7.92(ddd, 8.5, 2.5, 1.8)
H3'	7.65(ddd, 8.5, 2.5, 1.8)	7.27(d, 8.1)	7.51(ddd, 8.6, 2.5, 1.9)	8.12(dd, 8.6, 1.5)	7.62(dd, 8.2, 8.1)	7.51(ddd, 8.5, 2.5, 1.8)
H4'	–	–	–	7.98(d, 8.9)	8.05(d, 8.2)	–
H5'	7.65(ddd, 8.5, 2.5, 1.8)	7.27(d, 8.1)	7.51(ddd, 8.6, 2.5, 1.9)	7.95(m)	8.01(dd, 8.1, 1.3)	7.51(ddd, 8.5, 2.5, 1.8)
H6'	7.84(ddd, 8.5, 2.5, 1.8)	7.76(d, 8.1)	7.91(ddd, 8.6, 2.5, 1.9)	7.58(ddd, 8.9, 6.8, 2.1)	7.60(ddd, 8.1, 6.8, 1.0)	7.92(ddd, 8.5, 2.5, 1.8)
H7'	–	–	–	7.56(ddd, 8.9, 6.8, 2.1)	7.65(ddd, 8.3, 6.8, 1.3)	–
H8'	–	–	–	7.97(m)	8.27(dd, 8.3, 1.0)	–
3'-OMe	–	–	–	–	–	–
4'-OMe	–	–	–	–	–	–
4'-CH ₃	–	2.35(s)	–	–	–	–
	7	8	9	10	11	12
H2	7.60(d, 2.0)	7.60(d, 2.0)	7.61(d, 2.0)	7.61(d, 2.0)	7.61(dd, 2.6, 1.6)	7.61(d, 2.0)
H3	–	–	–	–	–	–
H4	–	–	–	–	7.76(ddd, 7.7, 1.6, 0.8)	–
H5	7.09(d, 8.5)	6.92(d, 8.4)	7.10(d, 8.5)	7.10(d, 8.5)	7.49(dd, 8.2, 7.7)	7.10(d, 8.5)
H6	7.91(dd, 8.5, 2.0)	7.67(dd, 8.4, 2.0)	7.91(dd, 8.5, 2.0)	7.88(dd, 8.5, 2.0)	7.24(ddd, 8.2, 2.6, 0.8)	7.90(dd, 8.5, 2.0)
2-OMe	–	–	–	–	–	–
3-OMe	3.857(s)	3.948(s)	3.86(s)	3.86(s)	3.85(s)	3.86(s)
4-OMe	3.87(s)	3.952(s)	3.87(s)	3.87(s)	–	3.87(s)
H α	7.82(d, 15.5)	7.63(d, 15.7)	7.98(d, 15.6)	7.68(d, 15.6)	7.93(d, 15.7)	7.71(d, 15.6)
H β	7.67(d, 15.5)	7.78(d, 15.7)	7.67(d, 15.6)	7.89(d, 15.6)	7.72(d, 15.7)	7.91(d, 15.6)
H1'	–	–	–	–	–	–
H2'	7.52(d, 1.8)	7.75(ddd, 8.9, 2.2, 2.0)	7.85(ddd, 8.5, 2.6, 1.9)	7.77(ddd, 8.1, 2.2, 2.0)	7.93(ddd, 8.6, 2.6, 1.9)	7.97(ddd, 8.8, 5.6, 3.0)
H3'	–	8.24(ddd, 8.9, 2.2, 2.0)	7.65(ddd, 8.5, 2.6, 1.9)	7.27(ddd, 8.1, 2.2, 2.0)	7.51(ddd, 8.6, 2.6, 1.9)	7.29(ddd, 8.8, 8.8, 3.0)
H4'	–	–	–	–	–	–
H5'	7.02(d, 8.4)	8.24(ddd, 8.9, 2.2, 2.0)	7.65(ddd, 8.5, 2.6, 1.9)	7.27(ddd, 8.1, 2.2, 2.0)	7.51(ddd, 8.6, 2.6, 1.9)	7.29(ddd, 8.8, 8.8, 3.0)
H6'	7.40(dd, 8.4, 1.8)	7.75(ddd, 8.9, 2.2, 2.0)	7.85(ddd, 8.5, 2.6, 1.9)	7.77(ddd, 8.1, 2.2, 2.0)	7.93(ddd, 8.6, 2.6, 1.9)	7.97(ddd, 8.8, 5.6, 3.0)
H7'	–	–	–	–	–	–
H8'	–	–	–	–	–	–
3'-OMe	3.86(s)	–	–	–	–	–
4'-OMe	3.82(s)	–	–	–	–	3.86(s)
4'-CH ₃	–	–	–	–	–	3.87(s)
	13	14	15	16	17	
H2	–	–	7.67(d, 2.0)	7.65(d, 2.0)	–	
H3	7.19(dd, 8.3, 0.7)	7.21(dd, 8.3, 0.9)	–	–	7.18(dd, 8.3, 0.4)	
H4	7.54(ddd, 8.3, 7.4, 1.8)	*7.58(ddd, 8.3, 7.4, 1.8)	–	–	7.52(ddd, 8.3, 7.4, 1.8)	
H5	7.06(ddd, 7.5, 7.4, 0.7)	7.07(ddd, 7.5, 7.4, 0.9)	7.12(d, 8.5)	7.12(d, 8.5)	7.05(ddd, 7.9, 7.4, 0.4)	

Table 1 (continued)

	13	14	15	16	17
H6	7.48(dd, 7.5, 1.8)	*7.53(dd, 7.6, 1.8)	7.94(dd, 8.5, 2.0)	7.96(dd, 8.5, 2.0)	7.45(dd, 7.9, 1.8)
2-OMe	3.86(s)	3.88(s)	–	–	3.85(s)
3-OMe	–	–	3.878(s)	3.878(s)	–
4-OMe	–	–	3.882(s)	3.884(s)	–
H α	7.34(d, 15.9)	*7.61(d, 16.0)	8.02(d, 15.3)	8.08(d, 15.5)	7.27(d, 16.0)
H β	7.47(d, 15.9)	*7.61(d, 16.0)	8.54(d, 15.3)	7.88(d, 15.5)	7.42(d, 16.0)
H1'	–	–	–	8.32(d, 1.5)	–
H2'	7.61(ddd, 8.1, 2.1, 2.0)	8.01(ddd, 8.9, 2.3, 2.0)	8.23(d, 7.3)	–	7.34(d, 2.0)
H3'	7.25(ddd, 8.1, 2.1, 2.0)	8.24(ddd, 8.9, 2.3, 2.0)	7.62(dd, 8.3, 7.3)	8.13(dd, 8.6, 1.5)	–
H4'	–	–	8.05(d, 8.3)	7.96(d, 8.6)	–
H5'	7.25(ddd, 8.1, 2.1, 2.0)	8.24(ddd, 8.9, 2.3, 2.0)	8.01(dd, 8.0, 1.6)	7.95(m)	6.99(d, 8.3)
H6'	7.61(ddd, 8.1, 2.1, 2.0)	8.01(ddd, 8.9, 2.3, 2.0)	7.60(ddd, 8.0, 6.8, 1.2)	7.58(ddd, 9.2, 6.9, 2.4)	7.26(dd, 8.3, 2.0)
H7'	–	–	7.65(ddd, 8.2, 6.8, 1.6)	7.56(ddd, 9.2, 6.9, 2.4)	–
H8'	–	–	8.27(dd, 8.2, 1.2)	7.98(m)	–
3'-OMe	–	–	–	–	3.81(s)
4'-OMe	–	–	–	–	3.80(s)
4'-CH ₃	2.34(s)	–	–	–	–

Table 2 ¹³C-NMR data of compounds 1–17

	1	2	3	4	5	6	7	8	9	10	11	12	13	14	15	16	17	
C1	130.3	130.6	130.5	130.5	130.4	130.4	130.8	130.9	130.4	130.6	138.9	130.5	128.9	128.3	130.5	130.5	129.3	
C2	131.0	130.9	131.0	130.9	131.0	110.8	110.8	111.0	110.8	110.8	113.1	110.8	157.6	158.1	110.9	110.8	157.4	
C3	114.0	114.0	114.0	114.0	114.1	148.8	148.8	149.7	148.8	148.8	159.6	148.8	112.3	112.5	148.9	148.9	112.3	
C4	163.3	163.2	163.3	163.2	163.3	153.3	153.1	154.0	153.3	153.2	121.1	153.3	132.9	133.6	153.4	153.3	132.5	
C5	114.0	114.0	114.0	114.0	114.1	110.9	110.8	110.2	110.9	110.9	129.9	110.9	120.5	120.6	111.0	110.9	120.5	
C6	131.0	130.9	131.0	130.9	131.0	123.5	123.3	123.5	123.5	123.3	119.3	123.4	129.4	129.8	123.5	123.5	129.2	
2-OMe	–	–	–	–	–	–	–	–	–	–	–	–	55.8	55.9	–	–	55.7	
3-OMe	–	–	–	–	–	55.6	55.6	56.4	55.6	55.6	55.4	55.6	–	–	55.6	55.6	–	
4-OMe	55.6	55.6	55.6	55.6	55.6	55.8	55.7	56.3	55.8	55.8	–	55.8	–	–	55.8	55.8	–	
C=O	187.2	187.4	187.2	187.3	187.3	187.2	187.3	187.8	187.2	187.3	188.8	187.3	192.2	191.6	187.3	187.3	192.5	
C α	122.8	121.0	122.8	122.3	124.5	122.7	119.6	125.7	122.8	120.9	122.8	121.9	126.0	130.6	124.6	122.3	125.0	
C β	141.7	143.2	141.6	143.1	139.0	141.6	143.5	140.9	141.7	143.1	142.6	141.8	142.7	139.2	139.0	143.1	143.5	
C1'	134.1	132.1	133.8	130.4	131.4	133.8	127.7	141.5	134.1	132.1	133.6	131.5	131.8	141.2	131.5	130.6	127.3	
C2'	130.7	128.8	130.5	132.5	125.5	130.5	111.1	129.0	130.7	128.8	130.6	131.1	128.5	129.5	125.6	132.5	110.8	
C3'	131.8	129.5	128.9	124.4	125.7	128.9	149.0	124.4	131.8	129.5	128.9	115.9	129.6	124.0	125.7	124.4	149.0	
C4'	123.7	140.5	134.9	128.4	130.6	134.8	151.1	148.6	123.7	140.4	135.2	163.3	140.5	148.0	130.6	128.4	151.1	
C5'	131.8	129.5	128.9	127.7	128.7	128.9	111.6	124.4	131.8	129.5	128.9	115.9	129.6	124.0	128.8	127.7	111.7	
C6'	130.7	128.8	130.5	127.3	126.2	130.5	123.5	129.0	130.7	128.8	130.6	131.1	128.5	129.5	126.3	127.3	123.0	
C7'	–	–	–	126.7	127.2	–	–	–	–	–	–	–	–	–	–	127.2	126.7	–
C8'	–	–	–	128.5	123.0	–	–	–	–	–	–	–	–	–	–	123.0	128.5	–
C9'	–	–	–	133.0	131.2	–	–	–	–	–	–	–	–	–	–	131.2	133.0	–
C10'	–	–	–	133.8	133.3	–	–	–	–	–	–	–	–	–	–	133.4	133.8	–
3'-OMe	–	–	–	–	–	–	3.86	–	–	–	–	–	–	–	–	–	55.6	
4'-OMe	–	–	–	–	–	–	3.82	–	–	–	–	–	–	–	–	–	55.6	
4'-CH ₃	–	21.1	–	–	–	–	–	–	–	–	–	–	21.0	–	–	–	–	

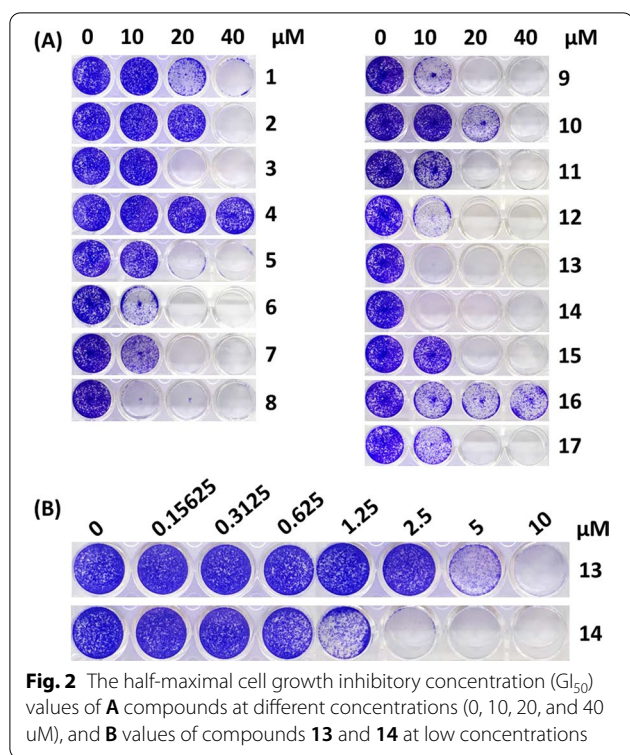


Table 3 The half-maximal cell growth inhibitory concentrations (GI_{50}) and mass spectra data of compounds **1–17**. All HR/MS data were collected in $[M+H]^+$ mode

Compound	Mass (M + H), (calcd./found)	GI_{50} , (μ M)
1	317.0177/317.0179	21.46 \pm 0.17
2	253.1229/253.1230	29.59 \pm 0.84
3	273.0682/273.0692	13.35 \pm 0.03
4	289.1229/289.1167	172.20 \pm 2.27
5	289.1229/289.1232	15.67 \pm 0.02
6	303.0788/303.0811	9.49 \pm 0.02
7	329.1389/329.1379	12.34 \pm 0.01
8	314.1028/314.1006	4.96 \pm 0.03
9	347.0283/347.0299	8.89 \pm 0.09
10	283.1334/283.1350	19.49 \pm 0.09
11	273.0682/273.0688	14.20 \pm 0.10
12	287.1083/287.1069	7.89 \pm 0.02
13	253.1229/253.1214	4.51 \pm 0.02
14	284.0923/284.0902	1.33 \pm 0.02
15	319.1334/319.1356	13.50 \pm 0.02
16	319.1334/319.1356	10.93 \pm 0.06
17	299.1283/299.1270	9.66 \pm 0.06

The GI_{50} values were determined using the densitometry and their values were in the range of 1.33 and 172.20 μ M. GI_{50} values and the mass spectra data of

chalcone compounds are listed in Table 3. The GI_{50} values with error bars were plotted against chalcone compounds (Additional file 1: Fig. S1).

To characterize why the compounds exhibit cell growth inhibitory effects against cancer cells, further biological experiments were performed. Because compound **14** showed the best GI_{50} value, it was selected for further biological experiments. Compound **14** showed a remarkable capacity on the cell viability inhibition of MCF-7SC after 24 and 48 h of treatment (Fig. 3A). Therefore, compound **14** was chosen to investigate the anti-cancer effects on stem like MCF-7SC cells in further experiments. Notably, Fig. 3B demonstrated that compound **14** could not cause cytotoxicity on fibroblast cells.

In addition, we checked whether compound **14** could induce apoptosis in MCF-7SC. Notably, compound **14** enhanced the proportion of the apoptotic population in MCF-7SC by 6.47% \pm 1.21% at a dose of 10 μ M, as shown by annexin V/propidium iodide staining (Fig. 4A, B). Furthermore, compound **14**-treated MCF-7SC cells displayed a decrease in the levels of caspase 7 and Bcl-2 while showing an increase of c-PARP, c-caspase 7, and Bax (Fig. 4C, D). Taking together, compound **14** exhibited the inhibitory potential on proliferation and apoptosis promotion of stem-like cell MCF-7SC.

MCF-7SC cells were previously reported to display greater stem cell characteristics and migratory potential compared to parental MCF-7 cells [19]. We next tested the effect of compound **14** on the migration of MCF-7SC cells. Figure 5A, B showed that compound **14** could prevent the MCF-7SC migrated cells at non-lethal concentrations after 12 and 24 h of exposure, as represented by wound healing assay. Epithelial-mesenchymal transition (EMT) has been involved in the stemness characteristic of CSCs. By losing adherent junctions and breaking down cell–cell interaction, EMT supported the metastatic initiating potential to further site in tumor cells [27]. Therefore, the efficiency of compound **14** on the levels of EMT markers was accessed by the western blot experiment. Markedly, compound **14** suppressed the levels of well-known mesenchymal markers such as Snail and Vimentin while increasing the level of an epithelial marker, E-cadherin dose-dependently, as shown in Fig. 5C, D.

CD44⁺/CD24⁻ population is considered as an important signature for breast CSC identification [28]. Interestingly, a dramatic decrease of this population was observed in MCF-7SC at dose 10 μ M by performing FACS analysis (77.94% \pm 4.51%) (Fig. 6A, B). Moreover, the levels of common stemness markers such as CD44, MRP1, and β -catenin were reduced after compound **14** treatment for 24 h, by 0.36 \pm 0.16, 0.72 \pm 0.11, and 0.52 \pm 0.07-fold, respectively (Fig. 6C, D). Abnormal activation of the transcriptional factor β -catenin, which is a

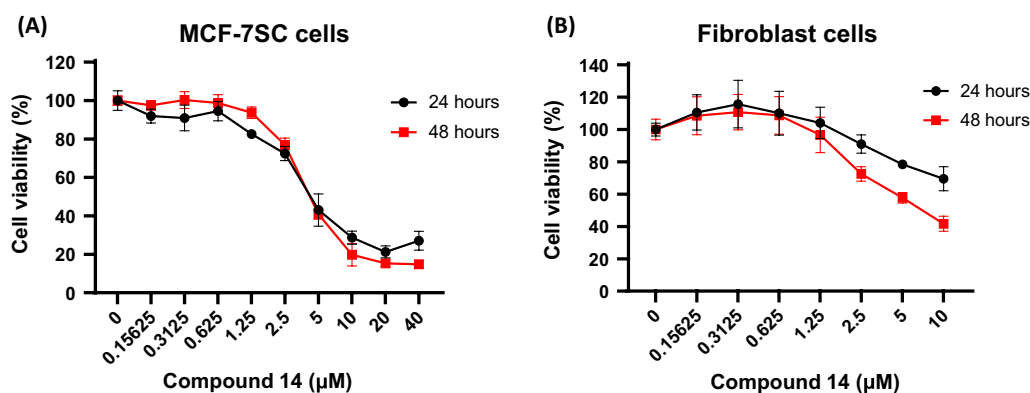


Fig. 3 Compound **14** inhibits proliferation of MCF-7SC cells. **A** The viability of MCF-7SC was evaluated by MTT assay following compounds **14** treatment for 24 and 48 h. **B** The cell viability of fibroblast cells was evaluated by MTT assay following compound **14** treatment for 24 and 48 h

crucial member of the Wnt signaling pathway, drives the pluripotency, self-renewal, and differentiation ability in CSCs, indicating the key pathway inhibitor as an attractive therapeutic target in cancer treatment [29]. Collectively, these results indicate that compound **14** could attenuate the stemness features of MCF-7SC cells.

To understand the results mentioned above at the molecular level, *in vitro* kinase assays were carried out using compound **14**. Several kinases known as targets for chemotherapy were selected: AMP-activated protein kinase, aurora kinase A, aurora kinase B, serine/threonine-protein kinase B-Raf, epidermal growth factor receptor, glycogen synthase kinase 3 beta, kinase insert domain receptor, mitogen-activated protein kinase, mammalian target of rapamycin, protein kinase A, and phosphoinositide 3-kinase. Compound **14** demonstrated 89% inhibitory activity at 10 µM against glycogen synthase kinase 3 beta (GSK3β).

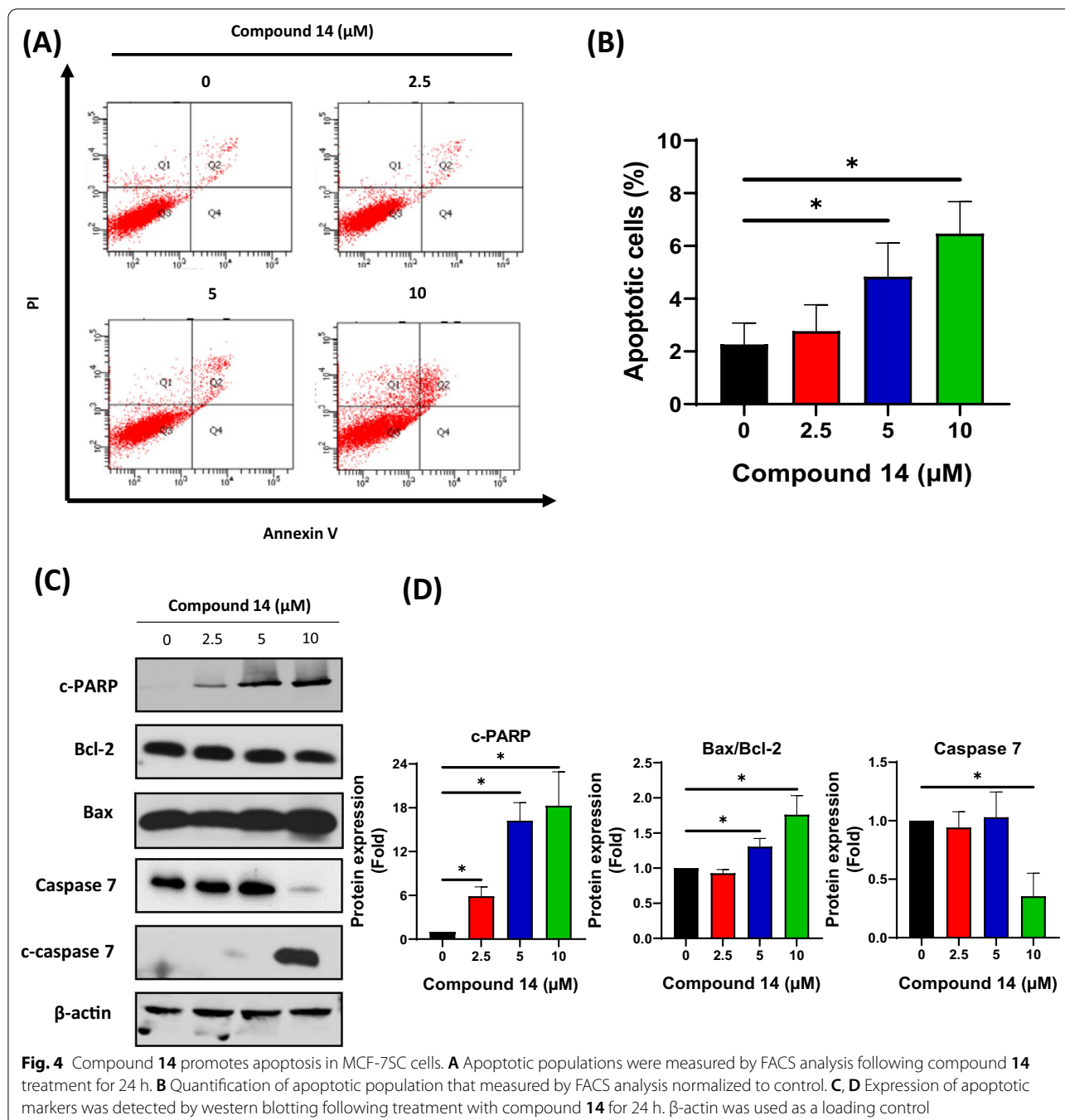
To elucidate whether compound **14** binds to GSK3β, *in silico* docking experiments were performed. As a 3D structure of GSK3β, the X-ray crystallographic structure deposited in the protein data bank as 5f95.pdb was used. It consists of two polypeptide chains, A and B. GSK3β is composed of 420 amino acids. Since chain A includes residues 36–383, and chain B does residues 36–385, chain B was selected for *in silico* docking. To prepare apo-protein a ligand, 2-[(cyclopropylcarbonyl)amino]-N-(4-phenylpyridin-3-yl)pyridine-4-carboxamide (named as 3up) contained in 5f95.pdb was deleted using the Chimera program. The binding pocket was determined using the grid box provided by AutoDock Tools as follows: the centers of x, y, and z were 55.361, 17.528, and 167.194, respectively, and the sizes of x, y, and z were 18, 20, and 20, respectively. To confirm whether this binding pocket is correct, the ligand, 3up contained in 5f95.pdb was docked into apo-protein using the AutoDock

vina program. Because the AutoDock program provides nine iteration docking process, nine complexes of GSK3β and 3up were generated. Their binding affinity ranged between -8.5 kcal/mol and -7.6 kcal/mol. Their docking poses were superposed with the X-ray crystallographic structure well. Next, compound **14** was tried to be docked into GSK3β apo-protein. Like the original ligand, 3up, nine complexes between GSK3β and compound **14** were generated. Their binding affinity ranged from -7.5 to -6.8 kcal/mol. Even their values were worse than those of the original ligand, as shown in Fig. 7A, B, the binding pose of compound **14** was superposed in a similar way.

The interactions between the residues of GSK3β and 3up (Fig. 8A) were compared with those between the residues of GSK3β and compound **14** (Fig. 8B) obtained using the LigPlot program. Eight residues were observed in both 3up and compound **14**: Ala83, Lys85, Leu132, Asp133, Tyr134, Val135, Leu188, and Asp200 where Asp200 shows a hydrogen bond with 3up but it does a hydrophobic interaction with compound **14**. While three residues including Ile62, Phe67, Val70 were observed in the GSK3β-compound **14** complex only, five residues including Pro136, Thr138, Arg141, Gln185, and Cys199 were observed in the GSK3β-3up complex. As a result, 13 residues participated in the interaction between GSK3β and 3up, but 11 residues did in compound **14**.

Different residues in the binding pockets of 3up and compound **14** may cause different binding poses as shown in Additional file 1: Fig. S2A, B. In addition, the original ligand, 3up made a hydrogen bond with the protein. These results demonstrate that the binding affinity of the original ligand should be lower than that of compound **14**.

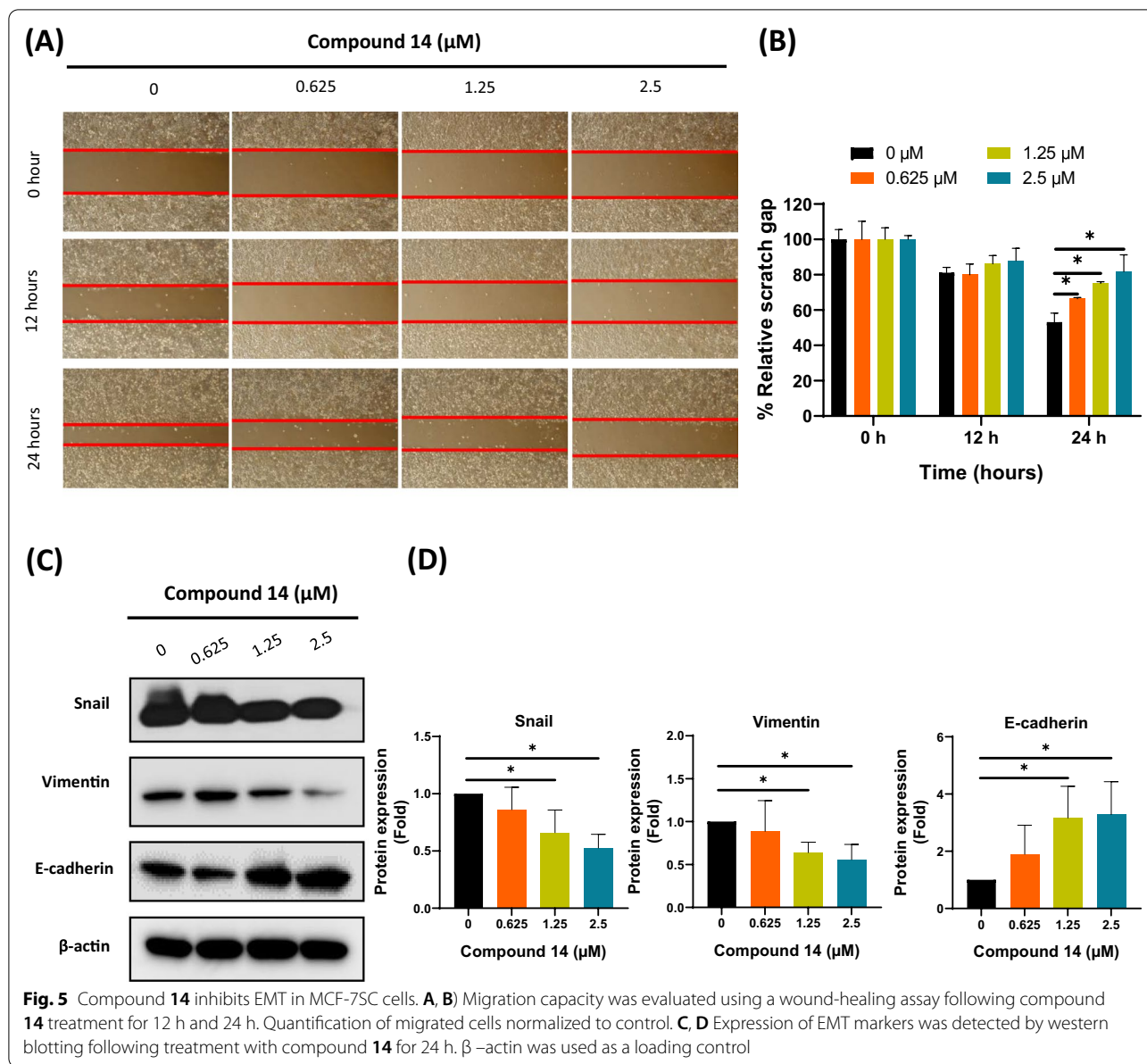
The druggability of compound **14** was evaluated using the SwissADME web tool provided by the Swiss Institute



of Bioinformatics (<https://www.sib.swiss/>). This compound does not violate Lipinski's rule [30]. It can show high gastrointestinal absorption and positive Blood-Brain Barrier penetration, and can have good bioavailability. The solubilities of the compounds were estimated based on the logP values calculated using the ChemDraw program (PerkinElmer, Arkon, OH, USA) and that of

compound 14 is logP=3.44. When a leadlikeness was evaluated based on combinatorial library, compound 14 did not violate any factors, so that it can be a lead compound as a chemotherapeutic agent [31].

Variouly substituted poly-methoxy chalcone compounds (1-17) were synthesized and their anticancer properties were confirmed. Long-term survival



clonogenic assay revealed that their GI50 values ranged between 1.33 and 172.20 μM. Treatment of MCF7SC cells with compound 14 at different concentrations reduced cell viability in a dose-dependent manner and induced apoptosis in MCF-7SC cells. Notably, the wound healing assay demonstrated that compound 14 prevented MCF-7SC migrating cells at non-lethal concentrations.

The anticancer-related mode of action was investigated through in vitro kinase assays, and it was confirmed that compound 14 inhibited the GSK3β enzyme. The binding mode of compound 14 to GSK3β was verified through in silico experiments, demonstrating that compound 14 binds to GSK3β with a binding affinity ranging from -7.5 kcal/mol to -6.8 kcal/mol.

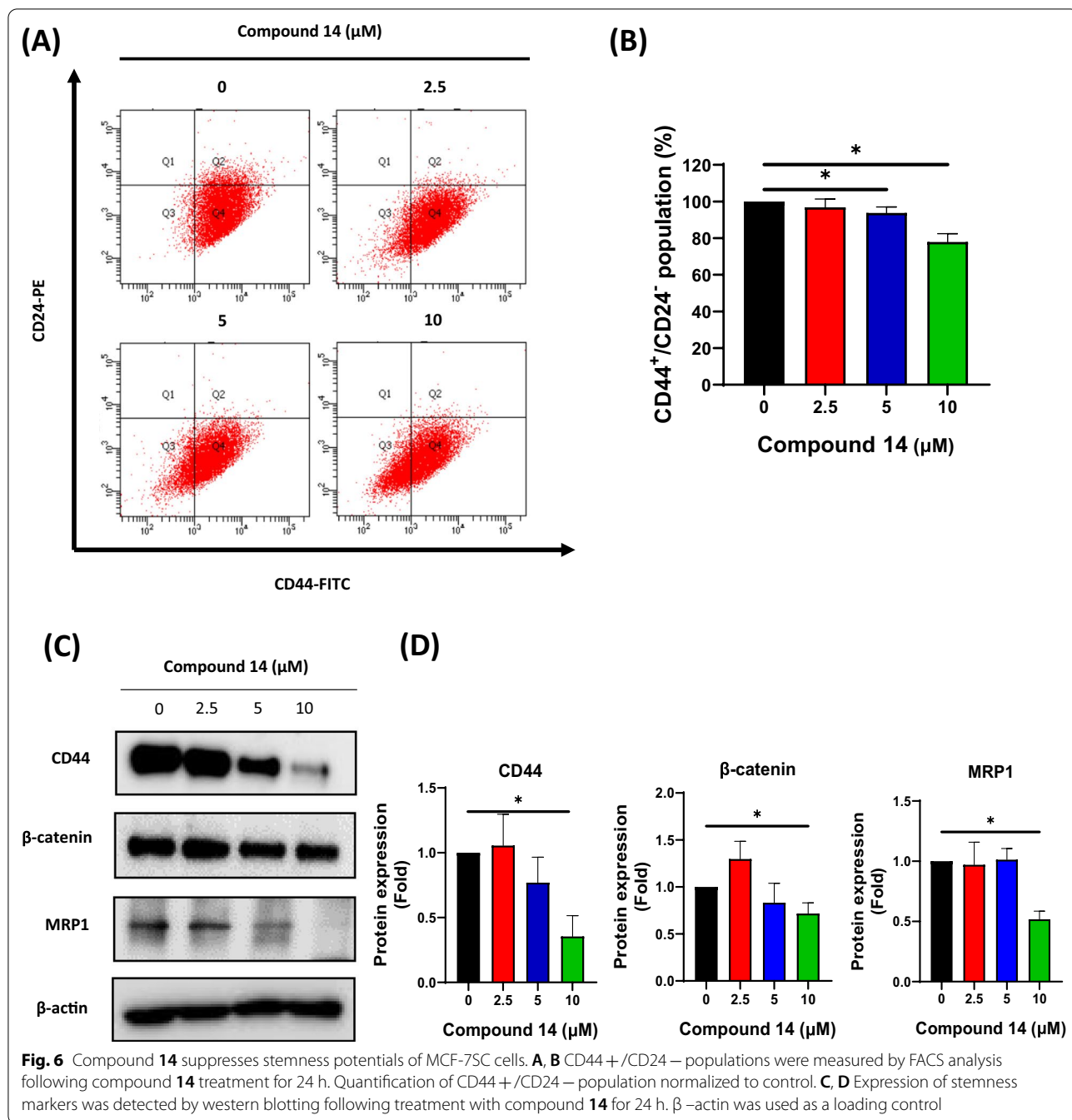


Fig. 6 Compound 14 suppresses stemness potentials of MCF-7SC cells. **A, B** CD44⁺/CD24⁻ populations were measured by FACS analysis following compound 14 treatment for 24 h. Quantification of CD44⁺/CD24⁻ population normalized to control. **C, D** Expression of stemness markers was detected by western blotting following treatment with compound 14 for 24 h. β -actin was used as a loading control

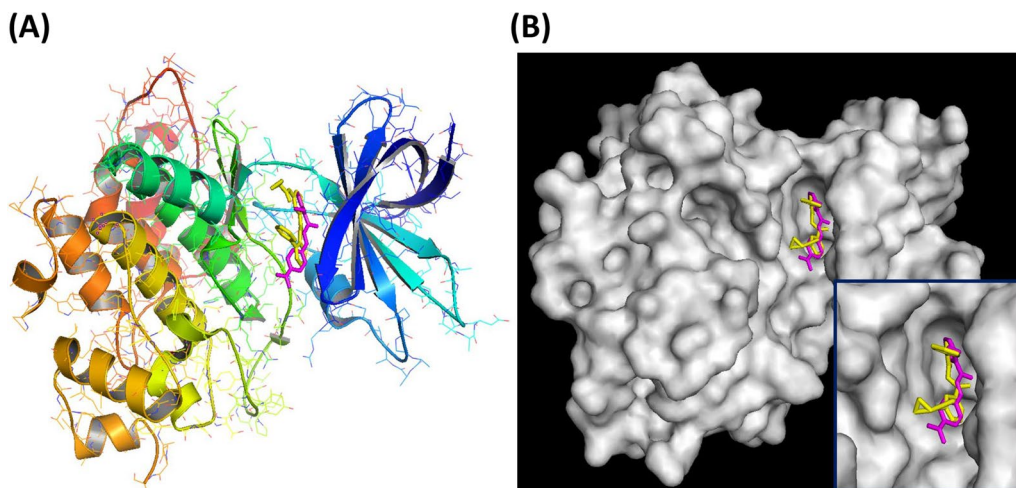


Fig. 7 **A** 3D image of the complex between GSK3β and the original ligand (yellow color) contained in 5f95.pdb (3up), and that between GSK3β and compound **14** (magenta color) generated by the PyMol program (The PyMOL Molecular Graphics System, Version 1.0r1, Schrödinger, LLC, Portland, OR). **B** 3D images of 3up (yellow color) and compound **14** (magenta color) inside the binding pocket which was enlarged and displayed in the box

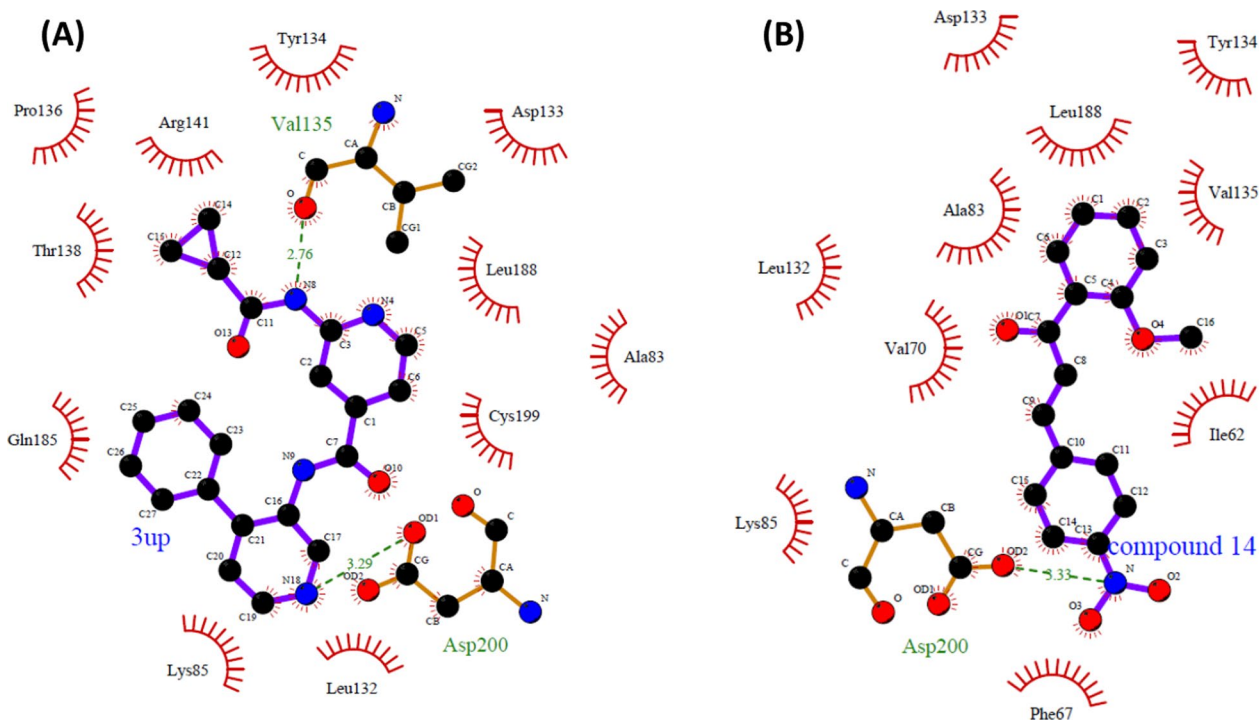


Fig. 8 **A** The interactions between the residues of GSK3β and 3up and **B** those between the residues of GSK3β and compound **14** obtained using the LigPlot program

Abbreviations

ABC: ATP binding cassette; ADME: Absorption distribution metabolism excretion; BCA: Bicinchoninic acid assay; CSC: Cancer stem cells; DMSO: Dimethyl sulfoxide; EMT: Epithelial-mesenchymal transition; FACS: Fluorescence-activated cell sorting; FITC: Fluorescein isothiocyanate; GSK3β: Glycogen synthase kinase 3 beta; HR/MS: High-resolution mass; MTT: 3-[4,5-Dimethylthiazol-2-yl]-2, 5-diphenyltetrazolium bromide sodium; MDR: Multidrug

resistance protein; MRP: Multidrug resistance-associated protein; NMR: Nuclear magnetic resonance; PBS: Phosphate-buffered saline; PE: Phytoerythrin; PMSF: Phenylmethylsulfonyl fluoride; PVDF: Polyvinylidene difluoride; RIPA: Radioimmunoprecipitation assay; ROS: Reactive oxygen species; TLC: Thin layer chromatography; SDS-PAGE: Sodium dodecyl sulphate–polyacrylamide gel electrophoresis.

Supplementary Information

The online version contains supplementary material available at <https://doi.org/10.1186/s13765-022-00686-x>.

Additional file 1: Fig. S1. The GI_{50} values with error bars plotted against chalcone compounds. **Fig. S2.** (A) 3D image of the residues surrounding the binding pocket of the original ligand, 3up, and (B) those of compound 14 generated using LigPlot and PyMol.

Acknowledgements

We appreciate the high-resolution mass spectrometry experiments conducted by Dr. Lee of Konkuk University.

Authors' contributions

Conceptualization, DK and SKC; Experiments, SA and VN-PT; Analysis, SA and BK; Investigation, SA and MY; Data Curation, VN-PT; Writing-Original Draft Preparation, DK and SKC; Writing-Review and Editing, YL and SKC; Supervision, DK. All authors read and approved the final manuscript.

Funding

The paper was supported by the Science Research Program through the National Research Foundation funded by the Ministry of Science and ICT, Republic of Korea (Grant no. NRF-2019R1F1A1058747).

Availability of data and materials

The datasets used and/or analyzed during the current study are available from the corresponding author on reasonable request.

Declarations

Ethics approval and consent to participate

Not applicable.

Consent for publication

The authors grants the publisher permission to publish the work in *Applied Biological Chemistry*.

Competing interests

The authors declare that they have no competing interests.

Author details

¹Department of Applied Chemistry, Dongduk Women's University, Seoul 02748, South Korea. ²Interdisciplinary Graduate Program in Advanced Convergence Technology and Science, Jeju National University, Jeju 63243, South Korea. ³Division of Bioscience and Biotechnology, Konkuk University, Seoul 05029, South Korea.

Received: 21 January 2022 Accepted: 27 February 2022

Published online: 14 March 2022

References

- Castaño LF, Cuartas V, Bernal A, Insuasty A, Guzman J, Vidal O, Rubio V, Puerto G, Lukáč P, Vimberg V, Balíková-Novtoná G, Vannucci L, Janata J, Quiroga J, Abonia R, Noguera M, Cobo J, Insuasty B (2019) New chalcone-sulfonamide hybrids exhibiting anticancer and antituberculosis activity. *Eur J Med Chem* 176:50–60
- Karimi-Sales E, Jeddi S, Ebrahimi-Kalan A, Alipour MR (2018) trans-Chalcone prevents insulin resistance and hepatic inflammation and also promotes hepatic cholesterol efflux in high-fat diet-fed rats: modulation of miR-34a-, miR-451-, and miR-33a-related pathways. *Food Funct* 9(8):4292–4298
- Inamullah F, Fatima I, Khan S, Kazmi MH, Malik A, Tareen RB, Abbas T (2017) New antimicrobial flavonoids and chalcone from *Colutea armata*. *Arch Pharm Res* 40(8):915–920
- Yadav N, Dixit SK, Bhattacharya A, Mishra LC, Sharma M, Awasthi SK, Bhasin VK (2012) Antimalarial activity of newly synthesized chalcone derivatives in vitro. *Chem Biol Drug Des* 80(2):340–347
- Mahapatra DK, Bharti SK, Asati V (2017) Chalcone derivatives: anti-inflammatory potential and molecular targets perspectives. *Curr Top Med Chem* 17(28):3146–3169
- Lee Y, Kim BS, Ahn S, Koh D, Lee YH, Shin SY, Lim Y (2016) Anticancer and structure-activity relationship evaluation of 3-(naphthalen-2-yl)-N,5-diphenyl-pyrazoline-1-carbothioamide analogs of chalcone. *Bioorg Chem* 68:166–176
- Shin SY, Lee JM, Lee MS, Koh D, Jung H, Lim Y, Lee YH (2014) Targeting cancer cells via the reactive oxygen species-mediated unfolded protein response with a novel synthetic polyphenol conjugate. *Clin Cancer Res* 20(16):4302–4313
- Shin SY, Kim JH, Yoon H, Choi YK, Koh D, Lim Y, Lee YH (2013) Novel anti-mitotic activity of 2-hydroxy-4-methoxy-2',3'-benzochalcone (Hymn-Pro) through the inhibition of tubulin polymerization. *J Agric Food Chem* 61(51):12588–12597
- Gil HN, Jung E, Koh D, Lim Y, Lee YH, Shin SY (2019) A synthetic chalcone derivative, 2-hydroxy-3',5',5'-trimethoxychalcone (DK-139), triggers reactive oxygen species-induced apoptosis independently of p53 in A549 lung cancer cells. *Chem Biol Interact* 298:72–79
- Gil HN, Koh D, Lim Y, Lee YH, Shin SY (2018) The synthetic chalcone derivative 2-hydroxy-3',5',5'-trimethoxychalcone induces unfolded protein response-mediated apoptosis in A549 lung cancer cells. *Bioorg Med Chem Lett* 28(17):2969–2975
- Heer E, Harper A, Escandor N, Sung H, McCormack V, Fidler-Benaoudia MM (2020) Global burden and trends in premenopausal and postmenopausal breast cancer: a population-based study. *Lancet Glob Health* 8:e1027–e1037
- Hu X, Huang W, Fan M (2017) Emerging therapies for breast cancer. *J Hematol Oncol* 10:98
- Prieto-Vila M, Takahashi RU, Usuba W, Kohama I, Ochiya T (2017) Drug resistance driven by cancer stem cells and their niche. *Int J Mol Sci* 18:2574
- Zhao J (2016) Cancer stem cells and chemoresistance: the smartest survives the raid. *Pharmacol Ther* 160:145–158
- Dandawate PR, Subramaniam D, Jensen RA, Anant S (2016) Targeting cancer stem cells and signaling pathways by phytochemicals: novel approach for breast cancer therapy. *Semin Cancer Biol* 40–41:192–208
- Butti R, Gunasekara VP, Kumar TV, Banerjee P, Kundu GC (2019) Breast cancer stem cells: biology and therapeutic implications. *Int J Biochem Cell Biol* 107:38–52
- Yang L, Shi P, Zhao G, Xu J, Peng W, Zhang J, Zhang G, Wang X, Dong Z, Chen F, Cui H (2020) Targeting cancer stem cell pathways for cancer therapy. *Signal Transduct Target Ther* 5(1):8
- Begiccevic RR, Falasca M (2017) ABC transporters in cancer stem cells: beyond chemoresistance. *Int J Mol Sci* 18(12):2362
- To NB, Nguyen YT, Moon JY, Ediriweera MK, Cho SK (2020) Pentadecanoic acid, an odd-chain fatty acid, suppresses the stemness of MCF-7/SC human breast cancer stem-like cells through JAK2/STAT3 signaling. *Nutrients* 12(6):1663
- Lee Y, Koh D, Lim Y (2018) 1 H and 13 C NMR spectral assignments of 25 ethyl 2-oxocyclohex-3-enecarboxylates. *Magn Reson Chem* 56(12):1188–1200
- Ahn S, Shin SY, Jung Y, Jung H, Kim BS, Koh D, Lim Y (2016) (1) H and (13) C NMR spectral assignments of novel flavonoids bearing benzothiazepine. *Magn Reson Chem* 54(5):382–390
- Shin SY, Yoon H, Hwang D, Ahn S, Kim DW, Koh D, Lee YH, Lim Y (2013) Benzochalcones bearing pyrazoline moieties show anti-colorectal cancer activities and selective inhibitory effects on aurora kinases. *Bioorg Med Chem* 21(22):7018–7024
- Trott O, Olson AJ (2010) AutoDock Vina: improving the speed and accuracy of docking with a new scoring function, efficient optimization, and multithreading. *J Comput Chem* 31(2):455–461
- Luo G, Chen L, Burton CR, Xiao H, Sivaprakasam P, Krause CM, Cao Y, Liu N, Lippy J, Clarke WJ, Snow K, Raybon J, Arora V, Pokross M, Kish K, Lewis HA, Langley DR, Macor JE, Dubowchik GM (2016) Discovery of

- isonicotinamides as highly selective, brain penetrable, and orally active glycogen synthase kinase-3 inhibitors. *J Med Chem* 59(3):1041–1051
25. Pettersen EF, Goddard TD, Huang CC, Couch GS, Greenblatt DM, Meng EC, Ferrin TE (2004) UCSF Chimera—a visualization system for exploratory research and analysis. *J Comput Chem* 25(13):1605–1612
 26. Lim Y, Koh, D (2013) *Acta Cryst E* 69: o514.
 27. Ribatti D, Tamma R, Annese T (2020) Epithelial-mesenchymal transition in cancer: a historical overview. *Transl Oncol* 13:100773. <https://doi.org/10.1016/j.tranon.2020.100773>
 28. Rabinovich I, Sebastião APM, Lima RS, Urban CA, Junior ES, Anselmi KF, Elifio-Esposito S, De Noronha L, Moreno-Amaral AN (2018) Cancer stem cell markers ALDH1 and CD44+/CD24- phenotype and their prognosis impact in invasive ductal carcinoma. *Eur J Histochem* 62(3):2943
 29. Zhang Y, Wang X (2020) Targeting the Wnt/ β -catenin signaling pathway in cancer. *J Hematol Oncol* 13:165
 30. Lipinski CA, Lombardo F, Dominy BW, Feeney PJ (2001) Experimental and computational approaches to estimate solubility and permeability in drug discovery and development settings. *Adv Drug Deliv Rev* 46(1–3):3–26
 31. Teague SJ, Davis AM, Leeson PD, Oprea T (1999) The design of leadlike combinatorial libraries. *Angew Chem Int Ed Engl* 38(24):3743–3748

Publisher's Note

Springer Nature remains neutral with regard to jurisdictional claims in published maps and institutional affiliations.

Submit your manuscript to a SpringerOpen[®] journal and benefit from:

- Convenient online submission
- Rigorous peer review
- Open access: articles freely available online
- High visibility within the field
- Retaining the copyright to your article

Submit your next manuscript at ► [springeropen.com](https://www.springeropen.com)
